INTERNATIONAL JOURNAL FOR NUMERICAL METHODS IN FLUIDS
Int. J. Numer. Meth. Fluids 2006; **50**:1085–1117
Published online 17 October 2005 in Wiley InterScience (www.interscience.wiley.com). DOI: 10.1002/fld.1087

Computational modelling of variably saturated flow in porous media with complex three-dimensional geometries

D. McBride[1,*,†], M. Cross[1,‡], N. Croft[1,§], C. Bennett[1,¶] and J. Gebhardt[2,‖]

[1]*School of Engineering, University of Wales Swansea, Swansea SA2 8PP, Wales, U.K.*
[2]*Process Engineering Resources Inc., 1945 South 1100 East, Suite 100, Salt Lake City, UT 84106, U.S.A.*

SUMMARY

A computational procedure is presented for solving complex variably saturated flows in porous media, that may easily be implemented into existing conventional finite-volume-based computational fluid dynamics codes, so that their functionality might be geared upon to readily enable the modelling of a complex suite of interacting fluid, thermal and chemical reaction process physics. This procedure has been integrated within a multi-physics finite volume unstructured mesh framework, allowing arbitrarily complex three-dimensional geometries to be modelled. The model is particularly targeted at ore heap-leaching processes, which encounter complex flow problems, such as infiltration into dry soil, drainage, perched water tables and flow through heterogeneous materials, but is equally applicable to any process involving flow through porous media, such as in environmental recovery processes. The computational procedure is based on the mixed form of the classical Richards equation, employing an adaptive transformed mixed algorithm that is numerically robust and significantly reduces compute (or CPU) time. The computational procedure is *accurate* (compares well with other methods and analytical data), *comprehensive* (representing any kind of porous flow model), and is *computationally* efficient. As such, this procedure provides a suitable basis for the implementation of large-scale industrial heap-leach models. Copyright © 2005 John Wiley & Sons, Ltd.

KEY WORDS: saturated-unsaturated flow; percolation flow; heterogeneous media; heap leaching

1. INTRODUCTION

The main objective of the work described here is the development and implementation of a three-dimensional numerical procedure for computational modelling of flow through variably saturated porous media. Developing robust, efficient numerical methods that handle a wide

*Correspondence to: D. McBride, School of Engineering, University of Wales Swansea, Swansea SA2 8PP, Wales, U.K.
†E-mail: D.Mcbride@swansea.ac.uk
‡E-mail: M.Cross@swansea.ac.uk
§E-mail: T.N.Croft@swansea.ac.uk
¶E-mail: C.R.Bennett@swansea.ac.uk
‖E-mail: jim@processing.com

Received 21 February 2005
Revised 1 August 2005
Accepted 2 August 2005

range of flow scenarios, i.e. variably saturated porous media domains that contain materials with spatially varying properties, infiltration into dry soil and perched water tables, has provided a computational challenge to the simulation community. There are a number of commercial software tools available that have been specifically designed for the solution of the three-dimensional Richards equation for porous flow problems; see, for example, the codes SWMS-3D [1], 3DFEMFAT [2], SVFLUX [3] and FEMWATER [4].

However, there are now a series of general-purpose commercial computational fluid dynamics (CFD) codes available (see, for example, References [5–7]), which enable a vast array of complex thermo-fluid physics to be represented. Thus, the objective of this paper is to develop a computational method for solving the variably saturated flow equations in the context of the computational environment typified by the generic CFD codes, so that their other features (i.e. well-established transport, thermal and chemical reaction procedures) might be utilized in comprehensive modelling of reactive porous-media-based processes, such as industrial heap-leaching processes [8]. Characterizing variably saturated flow within complex three-dimensional geometries represents a key stage in the development of a comprehensive model of heap leaching. In this work the variably saturated flow algorithm is implemented within PHYSICA, a general-purpose CFD computational modelling software frame work for multi-physics processes, based upon finite volume discretizations and expressed over three-dimensional unstructured meshes [9] with any mix of elements from tetrahedral to hexahedrals.

Flow through variably saturated porous media is characterized by the classical Richards equation combined with one of a number of laws to relate the pressure head to the moisture content of the porous medium. There are three standard forms of the Richards equations: h-based (pressure head), θ-based (moisture content) and 'mixed' form where both variables are employed:

(1) *The h-based form*, where the primary variable is the pressure head,

$$C(h)\frac{\partial h}{\partial t} = \nabla[K(h)\nabla h] + \frac{\partial K(h)}{\partial z} \tag{1}$$

where $C(h)$ is the specific moisture capacity, is defined as

$$C(h) = \frac{\partial \theta}{\partial h} \tag{2}$$

The h-based form allows for both unsaturated and saturated conditions. However, in highly non-linear problems, such as infiltration into very dry heterogeneous soils, these methods can suffer from mass-balance error, convergence problems and poor CPU efficiency. As discussed by Celia *et al.* [10], 'The reason for poor mass balance resides in the time derivative term'. While $\mathrm{d}\theta/\mathrm{d}t$ and $C(\mathrm{d}h/\mathrm{d}t)$ are mathematically equivalent in the continuous partial differential equation, their discrete analogues are not. The inequality in the discrete forms is exacerbated by the highly nonlinear nature of the specific capacity term $C(h)$. This leads to significant mass-balance errors in the h-based formulations because the change in mass in the system is calculated using discrete values of $\mathrm{d}\theta/\mathrm{d}t$ while the approximating equations use the expansion $C(h)(\mathrm{d}h/\mathrm{d}t)$. Using standard time-integration techniques, mass-balance errors grow with the time-step size. Various approaches have been developed to overcome the problem. Milly [11] proposed a mass-conserving solution that modifies the capacity term to force global mass balance. Pan *et al.* [12] proposed a mass-distributed scheme that satisfied mass balance and was oscillation free. Tocci *et al.* [13] have shown that using a differential algebraic

equation implementation of the method of lines results in good mass balance through time-step truncation-error control.

(2) *The θ-based form*, where the primary variable is the moisture content,

$$\frac{\partial\theta}{\partial t} = \nabla[D(\theta)\nabla\theta] + \frac{\partial K(\theta)}{\partial z} \tag{3}$$

where $D(\theta)$ is the hydraulic diffusivity. One of the advantages of the θ-based formulation is that perfectly mass conservative discrete approximations can be applied. However, this form degenerates under fully saturated conditions as heterogeneous material produces discontinuous θ profiles and a pressure–saturation relationship no longer exists [14].

(3) *The 'mixed' h–θ-based model*

$$\frac{\partial\theta}{\partial t} = \nabla[K(h)\nabla h] + \frac{\partial K(h)}{\partial z} \tag{4}$$

where both the moisture content and pressure head variables are employed in the solution. Numerical techniques that employ both θ and h in the solution procedure have been developed to minimize mass-balance errors and enhance computational efficiency. Kirkland *et al.* [15] defined a new variable, which is essentially the saturation in the unsaturated zone and the pressure in the saturated zone. Forsyth *et al.* [16] used a similar technique but employ variable substitution using a different primary variable in different regions. Diersch and Perrochet [17] used a primary variable switching technique, which is unconditionally mass conservative. This method involves assembling and solving an unsymmetric equation system at each time and iteration level which increases CPU time but reported faster convergence behaviour. Celia *et al.* [10] proposed a modified Picard iteration scheme that ensures mass balance by evaluating the moisture content change in a time step directly from the change in the water pressure head. It has been shown to provide excellent mass balance when modelling unsaturated problems with sharp wetting fronts [18]. This method is easy to implement into h-based codes, requiring only an additional source term. Huang *et al.* [19] proposed a computationally more efficient convergence scheme for the modified Picard iteration method based on using the pressure head as the primary variable. However, problems have been reported when employing the Celia *et al.* [10] mixed method form for free drainage problems [20, 21]. Hao *et al*. proposed a simple switching method between the mixed form modified Picard iteration scheme and the standard h-based Picard iteration scheme according to the local soil–water conditions. Hao *et al.* showed that the mass-balance error in the mixed form is closely related to the water capacity and time-step size. If relatively large values are encountered, mass-balance errors can accumulate with longer simulation times and larger domains. The h-based form can achieve good mass balance if the change in h is small enough during a time step whereas the mixed form improves mass balance with a sharp wetting front. Therefore, combining these, makes a more efficient procedure for long time simulations of water flow in soils with frequent infiltration and deep drainage processes. The method switches to the h-based form when the change in h is less than some prescribed value, otherwise the mixed form is applied.

Developing robust and efficient algorithms for certain flow problems, such as those that give rise to sharp wetting fronts, has provided a computational challenge to the simulation community. For this class of problem, small time-step sizes and a fine mesh is often required in order to maintain stability when steep wetting fronts develop, making large-scale multi-dimensional infiltration problems impractical to simulate. Since the solution changes in character with time,

employing a small time step-size not only adds significantly to CPU time, but also results in valuable computing time being spent on periods of simple solution behaviour with excessively small time steps [22]. In order to overcome the need for fine spatial and temporal discretization, transformation methods and adaptive grid algorithms [23–25] have been investigated by many authors. Employing local adaptive grid refinement into the numerical models can overcome the need for a fine mesh, but the computational cost is high and their introduction into three-dimensional codes is not trivial [26]. A number of authors have proposed mathematical transformations to reduce the nonlinearity of the equations, notably Haverkamp *et al.* [27], integral function, Ross [28], hyperbolic function, Kirkland *et al.* [15] and Forsyth *et al.* [16], variable switching, Pan and Wierenga [29], rational function and Williams *et al.* [30], a combined integral and water-content-based transformation. Transformations [15, 16, 27] are based, to some extent, on the soil hydraulic functions and vary spatially with media type. This dependency results in a discontinuity of the transformed variable in the case of heterogeneous media restricting their application to homogeneous media. Transformations [28–30] are continuous in heterogeneous media domains when constant transformation parameters are applied. Williams *et al.* [30] provided a comparison on the fore-mentioned transformations using fixed time-step methods and reported that their proposed combined integral method and the Pan and Wierenga transform function 'were able to provide accurate solutions at much larger discretization scales, resulting in very efficient simulations that would not be possible using untransformed RE or other transform methods investigated'. The combined integral method is a more complex approach, defined in terms of the moisture content and an integral of the hydraulic conductivity function.

$$h_t = \begin{cases} \displaystyle\int_{-\infty}^{h} K(h')\,\mathrm{d}h' + \beta[\theta(h) - \theta_r], & h \leqslant 0 \\ \left.\dfrac{\partial p}{\partial h}\right|_{h=0} {}^{*}h + h_t(0), & h > 0 \end{cases} \tag{5}$$

The Pan and Wierenga approach [29], uses a simple non-linear transformation, is easy to incorporate into computational algorithms and is not dependent on the hydraulic properties. The pressure head variable (h) is transformed into a new dependent variable (h_t),

$$h_t = \begin{cases} \dfrac{h}{1 + \beta h}, & h < 0 \\ h, & h \geqslant 0 \end{cases} \tag{6}$$

where β is a universal constant ($\cong -0.04\,\mathrm{cm}^{-1}$ or $-4\,\mathrm{m}^{-1}$) independent of both the $K(h)$ and $C(h)$ relationship.

Equation (4) now becomes

$$\frac{\partial \theta}{\partial t} = \nabla[K^*(h)\nabla h] + \frac{\partial K(h)}{\partial z} \tag{7}$$

where $\partial\vartheta/\partial t$ can be written as

$$\frac{\partial \vartheta}{\partial t} = \frac{\partial \vartheta}{\partial h}\frac{\partial h}{\partial h_t}\frac{\partial h_t}{\partial t} = C^*(h)\frac{\partial h_t}{\partial t} \tag{8}$$

$C^*(h)$ is the transformed specific water capacity, given as

$$C^*(h) = C(h)\frac{\partial h}{\partial h_t} = C(h)[1 + \beta h]^2 \tag{9}$$

$K^*(h)$ is the transformed hydraulic conductivity, given as

$$K^*(h) = K(h)\frac{\partial h}{\partial h_t} = K(h)[1 + \beta h]^2 \tag{10}$$

This transformation reduces the non-linearity of the hydraulic conductivity and volumetric water fraction as functions of the pressure head.

As observed by Mansell *et al.* [26] critical features of this method are that:

(1) Near saturation, $\beta h \ll 1$, so that $h_t = h$ for $h >= 0$
(2) For the specific case when $h = 0$, then $C^*(h) = 0$ and $K^*(h) = K_{\text{sat}}$ and the continuity for both h_t and $\partial h_t/\partial t$ is ensured at $h = 0$.
(3) For large negative values of h, then for vertical flow, $\partial h_t/\partial z < \partial h/\partial z$ which results in both faster convergence and less mass-balance error conditions involving large gradients of h.
(4) For zero and positive values of h then $\partial h_t/\partial z = \partial h/\partial z$ and $\partial h_t/\partial z > \partial h/\partial z$, respectively.

This transformation has been shown to significantly improve convergence and CPU efficiency, see References [29–32].

Williams and Miller [32] investigated the transformation methods [29, 30] together with adaptive time-stepping schemes for efficiency and robustness. Using an adaptive time-stepping scheme to adjust the time-step size improves convergence of the non-linear solution. They compared the empirically based adaptive time-stepping (EBATS) method [23] with Tocci *et al.*'s [13] differential algebraic equation-based method of lines (DAE/MOL). The EBATS approach is simple to implement into existing fixed time-step codes but requires the specification of a set of parameters for which there is no theoretical guidance. Nevertheless, EBATS has been commonly employed in a number of codes, such as SWMS-2D [33], FEMWATER [34] and HYDRUS [35] to improve efficiency and robustness. The DAE/MOL approach estimates temporal truncation error to explicitly control the solution order and time-step size. Williams *et al.* reported DAE/MOL to be generally more effective than the EBATS method for high levels of accuracy but it is not so straightforward to implement in general-purpose CFD codes.

In a recent review, Mansell *et al.* [26] summarize the use of adaptive-grid-refinement techniques to capture the moisture interface with appropriate levels of precision for numerical simulation. They identify two main ways of addressing the challenge posed by the moving boundary at the moisture interface. One concerns the transformation of the original equations so that the discontinuity is smoothed out in some way, whilst the second involves the use of adaptive-grid-refinement techniques. The second is undesirable in modelling reactive transport in porous media (such as, heap leaching) because there is so much else going on in terms of gaseous flow, chemical reactions and thermal transport, that a fixed-grid solution is much preferred if a suitably accurate procedure can be identified. The fixed-grid route is the standard route for the solution of another class of moving boundary problems, solidification and melting, see, for example, Reference [36, 37] where very convoluted flow physics occurs within complex three-dimensional geometries. At the phase change from liquid to solid

there is a discontinuity in the thermal gradient due to the latent heat evolution or consumption and capturing this feature numerically presents a significant challenge. However, in these equations, the enthalpy rather than the temperature is normally solved for and conserved—this physical variable varies smoothly across the phase-change region, and therefore presents no particular challenges to the numerical procedures. Coupled with suitable temperature–-fraction solid relationships, all the physical variables of interest can be recovered and tracked in a numerically robust fashion using a fixed-grid approach. Employing a transformation method appears to provide the potential for a similar kind of solution route for solving variably saturated flow in complex porous domains in a manner similar to that of solidification/melting moving boundary problems.

There are wide ranges of techniques and discretization methods employed in a variety of ways in the solution of the Richards equations. For example, Huang *et al.* [38] use an adaptive moving mesh and finite element discretization, Manzini and Ferraris [39] investigate mass conservative finite volume methods on two-dimensional unstructured grids, Voller [40] employs Celia's [10] mass conservative scheme using the control volume finite element (i.e. unstructured mesh) method. Rees *et al.* [41] employs Forsyth *et al.* [16] variable substitution technique using an edge-based finite volume scheme. In both of these cases, the variable is solved for at the vertex of each cell or element. In this work we report an effective and robust procedure, where the variables are solved at the cell/element centre and which can easily be implemented into a conventional finite-volume-based CFD code. The Pan and Wierenga [29] transformation was chosen for its simplicity and ability to provide solutions at relatively large discretization scales. The mixed form of the Richards equation is solved, employing the 'Celia linearization' [10] to ensure mass balance and the simple switching Picard iteration scheme [21] to improve solutions for free drainage problems. The algorithm allows for either the Brooks–Corey [42] or the van Genuchten [43] pressure-head–moisture relationships to be employed. A simple empirical adaptive time-stepping scheme was used, not only for its ease of implementation, but also for its ability to improve computational efficiency and solution robustness. This computational approach is implemented and tested within PHYSICA, a general-purpose CFD computational modelling software framework for multi-physics processes [44]. This code uses a three-dimensional finite volume formulation expressed on an unstructured mesh framework with conventional cell-centred discretizations and appropriate interpolations to ensure flux conservation across the cell faces, as might be found in any of the leading general-purpose CFD codes.

2. THE BASIC MATHEMATICAL MODEL: FORMS OF THE RICHARDS EQUATION AND PRESSURE-HEAD–MOISTURE-CONTENT RELATIONSHIPS

The Richards equation is written in terms of the water pressure head and the water moisture variables, and is defined by coupling the flow continuity equation with the Darcy flux equation.

2.1. Variables

The main variables used to describe the movement of moisture through variably saturated regions are:

The pressure head or capillary head (h) defined as

$$h = \frac{P}{\rho g} \tag{11}$$

where P is the pressure, ρg is the specific weight of water. In unsaturated regions h will take negative values due to capillary suction. In saturated regions all voids are filled with moisture and $h \geqslant 0$.

The total hydraulic head (H) is

$$H = h + z \tag{12}$$

where z is the elevation head, with the vertical distance assumed upwards.

The moisture content (θ) takes the saturated value, θ_{sat}, in saturated regions and in unsaturated regions is dependent upon h, giving $\theta_{\text{res}} < \theta(h) < \theta_{\text{sat}}$, where θ_{res} is the residual moisture content of the material.

2.2. The volumetric flow rate

The Darcy equation describes the movement of moisture in saturated porous flow,

$$q_{x_i} = -K_{\text{sat}} \frac{\partial H}{\partial x_i} \tag{13}$$

where q is the flux in the x_i direction and K_{sat} is the saturated hydraulic conductivity.

For unsaturated porous flow, Equation (13) is modified so that the hydraulic conductivity is expressed as a function of the pressure head,

$$q_{x_i} = -K(h) \frac{\partial H}{\partial x_i} \tag{14}$$

To ensure mass conservation, the volumetric continuity equation also needs to be satisfied.

$$\frac{\partial \theta}{\partial t} = -\frac{\partial q_x}{\partial x} - \frac{\partial q_y}{\partial y} - \frac{\partial q_z}{\partial z} \tag{15}$$

Substituting (14) into (15) and rewriting in terms of the pressure head (h) gives the mixed form of the Richards equation (4).

2.3. Pressure-head—moisture-content relationship

The mixed form of the Richards equation (4), is written in terms of two unknown variables, moisture content (θ) and pressure head (h). Hence, to complete the model for variably saturated flow, constitutive relationships for pressure-head–moisture-content–hydraulic-conductivity need to be specified. The most commonly employed models by the community and used within in this work, are given below.

Brooks–Corey [42]

$$\theta = \begin{cases} (\theta_{\text{sat}} - \theta_{\text{res}})(h/h_d)^{-n} + \theta_{\text{res}}, & h < h_d \\ \theta_{\text{sat}}, & h \geqslant h_d \end{cases} \tag{16}$$

$$K = K_{\text{sat}} \left[\frac{\theta - \theta_{\text{res}}}{\theta_{\text{sat}} - \theta_{\text{res}}} \right]^{3+2/n} \tag{17}$$

van Genuchten [43]

$$\theta = \begin{cases} \theta_{\text{res}} + \dfrac{\theta_{\text{sat}} - \theta_{\text{res}}}{[1 + |\alpha h|^n]^m}, & h < 0 \\ \theta_{\text{sat}}, & h \geqslant 0 \end{cases} \tag{18}$$

$$K = K_{\text{sat}} \left[\frac{\theta - \theta_{\text{res}}}{\theta_{\text{sat}} - \theta_{\text{res}}} \right]^{0.5} \left[1 - \left(1 - \left[\frac{\theta - \theta_{\text{res}}}{\theta_{\text{sat}} - \theta_{\text{res}}} \right]^{1/m} \right)^m \right]^2 \tag{19}$$

where and α and n are material parameters which affect the shape of the soil hydraulic functions and $m = 1 - 1/n$, $h_d = -1/\alpha$.

The unsaturated soil hydraulic properties $\theta(h)$ and $K(h)$ are in general highly nonlinear functions of the pressure head. It is this highly nonlinear dependency of the hydraulic properties on the pressure head makes solution of the Richards equation problematic, and requiring a sophisticated numerical scheme, such as the one described below.

3. NUMERICAL FORMULATION—FINITE VOLUME DISCRETIZATION ON AN UNSTRUCTURED MESH

In order to solve the governing partial differential equation for variably saturated flow, a finite volume discretization scheme is employed. The solution domain is divided into a number of non-overlapping finite control volumes (i.e. elements) and the governing equation is integrated over each control volume as well as over time. This method ensures that mass conservation is enforced locally by means of consistent expressions for fluxes through the faces of adjacent control volumes. The approach is usually described over structured meshes in most conventional CFD-based texts, see Reference [45], but has now been extended to arbitrarily structured meshes, and is used as the basis for most of the leading commercial CFD codes [6–8]. In these software technologies, and in that employed here, the hydraulic variables are solved at the centre of the cell. Special care is taken to avoid oscillatory solutions for Navier–Stokes flows, typically through the use of Rhie–Chow-type approximations [46] when calculating the element-face fluxes. For porous flow calculations the fluxes are evaluated directly from adjacent element pressure values. However, there may be ambiguity in evaluating the face hydraulic conductivity values, k_f, at an interface between control volumes. Its value could be calculated using an arithmetic mean or a harmonic mean. For converging solutions it was

found that an arithmetic mean was required in the solution of the transformed Richards equation but in calculating the inter-nodal flux the transformation actually modifies the way k_f is calculated. Applying the transformation to Darcy's law, the vertical flux, $q_{j+1/2}$, at an interface of two control volumes (i,j) and $(i,j+1)$ can be written as

$$q_{j+1/2} = 0.5\left[k_j\left(\frac{\partial h}{\partial h_t}\right) + k_{j+1}\left(\frac{\partial h}{\partial h_t}\right)_{j+1}\right]\left[\frac{(h_t)_{j+1} - (h_t)_j}{h_{j+1} - h_j}\right]\left[\frac{h_{j+1} - h_j}{\partial z}\right] - 0.5(k_j + k_{j+1}) \quad (20)$$

where the gravity term is evaluated using simple averaging.

Applying the transformation shown in Equation (6), the inter-nodal vertical flux can be expressed as

$$q_{j+1/2} = 0.5\left[k_j\frac{(1+\beta_j h_j)}{(1+\beta_{j+1}h_{j+1})} - k_{j+1}\frac{(1+\beta_{j+1}h_{j+1})}{(1+\beta_j h_j)}\right]\left[\frac{h_{j+1} - h_j}{\partial z}\right] \times \left[\frac{1 + h_{j+1}h_j(\beta_j - \beta_{j+1})}{h_{j+1} - h_j}\right] - 0.5(k_j + k_{j+1}) \quad (21)$$

Note that the third term on the right-hand side is zero when adjacent control volumes are either unsaturated or saturated (when $\beta_j = \beta_{j+1}$) but is non-zero on an interface between saturated and unsaturated regions.

Using a cell-centred unstructured mesh fully implicit formulation, the discretized form of the h-based, Equation (1), for a control volume, P, is

$$\frac{V_P}{\Delta t}C(h)(h - h^0) = \sum_f K(h)_f A_f \frac{(h_A - h_P)}{d_f} + \sum_f A_f K(h)_f n_f^z \quad (22)$$

and for the mixed form, Equation (4), is

$$\frac{V_P}{\Delta t}(\theta - \theta^0) = \sum_f K(h)_f A_f \frac{(h_A - h_P)}{d_f} + \sum_f A_f K(h)_f n_f^z \quad (23)$$

where superscript 0 indicates the value at a previous time step, subscript A indicates the value in the adjacent control volume, f is the face of the control volume, n the outward normal vector, d_f the distance across the control volume face, V_P the volume, A_f the cell face area, Δt is the time interval and $K(h)_f$ is evaluated using an arithmetic mean.

The mixed form ensures mass balance by separating the moisture content term into two parts during the iterative solution process, as proposed by Celia *et al.* [10],

$$\frac{V_P}{\Delta t}(\theta - \theta^0) = \frac{V_P}{\Delta t}C(h)(h^{n+1} - h^n) + \frac{V_P}{\Delta t}(\theta^n - \theta^0) \quad (24)$$

where $n+1$ and n denote the current and previous iteration levels, respectively. The second term on the right-hand side of (24) is known prior to the current iteration and enters the discretized equation as a source,

Applying transformation (6) to Equation (22) the discretized equation is now,

$$\frac{V_P}{\Delta t}C^*(h)(h_t^{n+1} - h_t^0) = \sum_f K^*(h)_f A_f \frac{(h_{tA}^{n+1} - h_{tp}^{n+1})}{d_f} + \sum_f A_f K(h)_f n_f^z \quad (25)$$

and for Equation (23),

$$\frac{V_P}{\Delta t} C^*(h)(h_t^{n+1} - h_t^n) = \sum_f K^*(h)_f A_f \frac{(h_{t_A}^{n+1} - h_{t_p}^{n+1})}{d_f} + \sum_f A_f K(h)_f n_f^z + \frac{V_P}{\Delta t}(\theta^0 - \theta^n) \qquad (26)$$

where $C^*(h)$ is the transformed specific water capacity, Equation (9) and $K^*(h)$ is the transformed hydraulic conductivity, Equation (10).

The solution, in a time step, of the non-linear Equations (25) and (26) is achieved by using an iterative solution strategy with all non-linear terms being evaluated at the previous iteration level. Applying the switching method [21], the absolute value of the pressure head change, h_c, within a time step is calculated as

$$h_c = (|h^{n+1} - h^0|) \qquad (27)$$

If h_c is below a specified threshold value, h_0, the h-based form (25) is solved, otherwise the mixed form (26) is solved. The default value of h_0 is 3 cm.

The solution procedure is started by obtaining initial values for h, $C(h)$ and $K(h)$. The initial values are obtained from the pressure-head–moisture-content–hydraulic-conductivity relationship, Equations (16)–(19), from initial pressure or moisture values. Initially, the h-based form, Equation (25) is solved.

Within a time step the implicit solution strategy is as follows:

1. Calculate $C(h)$ and $K(h)$ using (16)–(19).
2. Apply transformation (6) to the pressure head field to obtain h_t.
3. Obtain $C^*(h)$ and $K^*(h)$ from (9) and (10).
4. Obtain new h_t field: If ($h_c < h_0$) solve (25), else solve (26).
5. Apply inverse transformation of (6) to obtain new pressure head field.
6. Update moisture content using (16) or (18).
7. Calculate control volume face fluxes using (21), * if required.
8. Calculate h_c (27) and if not converged, repeat 1–8.

NOTE*: The face fluxes (21) do not form part of the pressure-head–moisture-content solution procedure but are required when solving other transported quantities.

As highlighted above, the h_t transform is free from the difficulties commonly experienced for heterogeneous materials and with hysteresis problems of the θ-based version of the Richards equation. As such, it has the potential to be both rapidly converging and also to provide accurate solutions to problems with sharp discontinuities.

4. IMPLEMENTATION OF THE VARIABLY SATURATED POROUS MEDIA FLOW PROCEDURE AS A PHYSICA MODULE

PHYSICA provides a three-dimensional finite volume unstructured mesh modular framework for multi-physics modelling [9, 44]. The framework supplies generic routines to discretize a general transport equation over a solution domain using cell-centred approximations over an arbitrarily complex three-dimensional mesh comprised of a mix of tetrahedral, wedge and hexahedral elements. Aside from a range of linear solvers, additional physical relations, such as the pressure-head–moisture relationships may be implemented through user routines.

A general module for solving variably saturated flow has been implemented into the host code, PHYSICA. The default method is outlined above; i.e. it uses the mixed form of the Richards equations, where both the moisture content and pressure head variables are employed in the solution of Equation (4), with the pressure head as the primary variable. The method proposed by Celia *et al.* [10] can be employed to capture the moisture change in a time interval and to ensure mass conservation or the switching method proposed by Hao *et al.* [21] for free drainage problems. A default value of 3 cm is used for the change in h within iteration for switching between h-based and mixed form. The mathematical transformation of Pan and Wierenga [29] is applied to the governing equations to overcome numerical difficulties associated with highly non-linear hydraulic properties. A default value of $-4\,\mathrm{m}^{-1}$ is used for the transformation parameter, β, although an option to change it is included. The van Genuchten [43] pressure–moisture relationship has been selected as the default value, although again, the Brooks–Corey [42] relationship has also been implemented and can be selected. An adaptive time-stepping scheme is used to optimize convergence and CPU efficiency. Options on the following models have been implemented within the module using a finite volume discretization over a three-dimensional unstructured mesh:

- Solve 'mixed-form' or 'h-based' equation or 'switch'.
- Solve 'classical' or 'transformed' equation.
- Select 'van Genuchten' or 'Brooks–Corey' model.

So that a wide range of approaches can be evaluated on all the test problems.

The host code solves a general conservation equation using cell-centred finite volume discretization techniques over an unstructured three-dimensional mesh. The conservation equation can be expressed by

$$\frac{\partial(T_\phi \phi)}{\partial t} + \mathrm{div}(C_\phi \underline{u}\phi) = \mathrm{div}(D_\phi \,\mathrm{grad}(\phi)) + S\phi \tag{28}$$

The general equation is integrated over each control volume as well as over time. Through the discretization procedure each term is approximated to produce a system of linear equations of the form $[A][\phi] = [B]$, where $[\phi]$ is a vector of values of ϕ at a number of finite points in the solution domain. The host code includes non-linear iterative solution techniques and a number of linear solver techniques, over-relaxed Jacobi (JOR), over-relaxed Gauss Seidel (SOR), pre-conditioned conjugate gradient (JCG), pre-conditioned bi-conjugate gradient (BICG), bi-conjugate gradient stabilized, (BICGSTAB) and GMRES. The JCG linear solver was employed for the test problems shown.

The porous flow module is initiated by setting $\phi = h_t$ and the coefficients in the general equation, $T_\phi = C^*(h)$, $D_\phi = K^*(h)$ and $C_\phi = 0$, giving a discretized transformed h-based Equation (25), for a control volume P with adjacent control volume A,

$$\frac{V_P}{\Delta t} C^*(h)(h_{tP}^{n+1} - h_{tP}^0) = \sum_f K^*(h)_f A_f \frac{(h_{tA}^{n+1} - h_{tp}^{n+1})}{d_f} + \sum_f A_f K(h)_f n_f^z + S_h \tag{29}$$

where the superscript 0 indicates the value at the previous time step and n is the iteration level. Equation (29) can easily be adjusted to the transformed mixed form, Equation (26), by setting h_t^0 to h_t^n in each iterative sweep and including an extra source term based on the

change in moisture content

$$S_h = \frac{V_p}{\Delta t}(\theta^n - \theta^0) \tag{30}$$

This simple adjustment from h-based to mixed form allows a switching algorithm to be employed, solving the h-based form when the change in the pressure within a time step is small and solving the mixed form when sharp changes occur.

Using a locally conservative finite volume formulation combined with a Taylor series development in time of the water content dependent variable ensures that all converging solutions are mass conservative. To improve CPU efficiency a simple adaptive time-step strategy has been implemented into the procedure here. This method monitors convergence during the simulation and identifies an optimum time increment for the solution time period. The simulation starts with a specified initial time increment, Δt. This time increment is automatically adjusted at each time period according to the following rules:

1. if $m_1 \leqslant m \leqslant m_2$, then $\Delta t_{n+1} = \Delta t_n$
2. else if $m < m_1$, then $\Delta t_{n+1} = \min(f_t \Delta t_n,\ \Delta t_{\max})$
3. else if $m > m_2$, then $\Delta t_{n+1} = \max(\Delta t_n / f_t,\ \Delta t_{\min})$

where m is the number of iterations required to converge for time step n, m_1 a lower iteration limit, m_2 an upper iteration limit, f_t a time-step acceleration factor, $\Delta t_{\max}$ the maximum allowable time-step size and $\Delta t_{\min}$ the minimum allowable time-step size.

5. EVALUATION OF THE SOLUTION PROCEDURE ON SOME DISCRIMINATING TEST PROBLEMS

In order to test and evaluate the solution procedure outlined above, the method is applied to a number of one- and two-dimensional test cases and compared to results available in the literature. The one-dimensional test cases involve flow into a layered soil with variable initial conditions: moist, intermediate and very dry [29] and a drainage case with initially saturated conditions [47]. The two-dimensional test cases [15, 17, 29] involve flow into very dry heterogeneous soil. The first case is unsaturated flow resulting in variably saturated conditions. In the second case, a perched water table develops surrounded by unsaturated soil. These cases represent good challenges for a numerical algorithm due to their highly non-linear nature. Finally, the procedure is applied to a three-dimensional geometry that is of significance for application to industrial heap leaching.

5.1. Problem 1: one-dimensional flow into a layered soil

The soil profile has soil 1 (sand) from 0 to 50 cm and 90 to 100 cm, and soil 2 (clay) from 50 to 90 cm. The hydraulic properties of the soils are given in Table I. The van Genuchten model is used to prescribe the pressure–moisture relationship. The initial and boundary conditions and simulation times are given in Table II. Cases 1.1–1.3 involve purely unsaturated flow and Cases 2.1–2.3 are for variably saturated flow with a perched water table.

The plots of the steady-state moisture content, Figure 1 for unsaturated flow and Figure 2 for variably saturated flow, are in good agreement with the published results [29]. The simulations

Table I. Hydraulic properties for soils 1 and 2 (Case 5.1).

	Soil 1	Soil 2
θ_{sat}	0.3658	0.4686
θ_{res}	0.0286	0.1060
$\alpha\,\mathrm{cm}^{-1}$	0.0280	0.0104
N	2.2390	1.3954
K_{sat} (m/s)	6.26×10^{-3}	1.5167×10^{-4}

Table II. Initial and boundary conditions (Case 5.1).

Case	Initial condition	Upper flux (m/s)	Lower flux (m/s)	Simulation time (h)
1.1	Moist	8.333×10^{-7}	0.0	4
1.2	Moderate	8.333×10^{-7}	0.0	8
1.3	Very dry	8.333×10^{-7}	0.0	12
2.1	Moist	3.472×10^{-6}	0.0	3.8
2.2	Moderate	3.472×10^{-6}	0.0	5
2.3	Very dry	3.472×10^{-6}	0.0	6

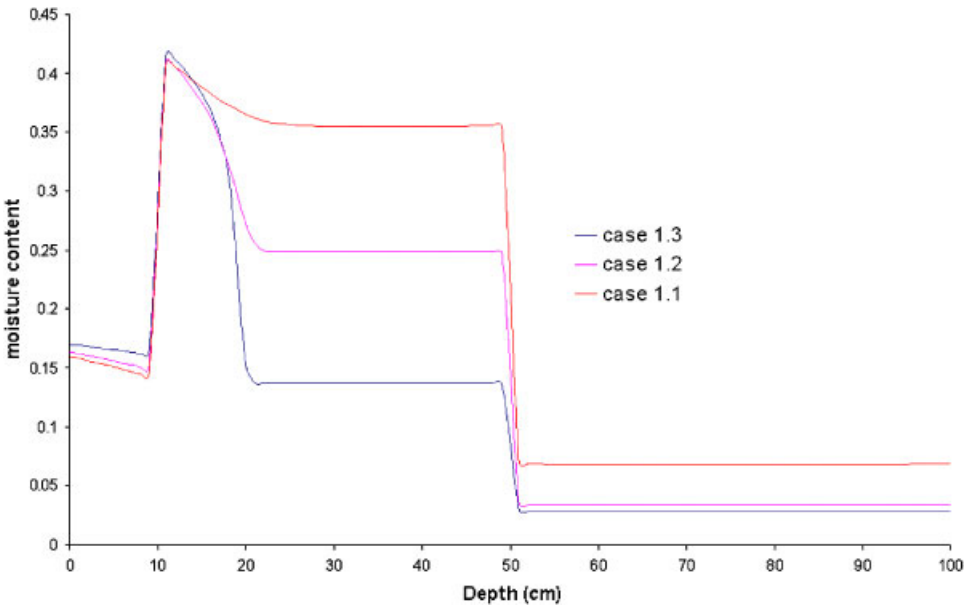

Figure 1. One-dimensional unsaturated flow (Case 5.1).

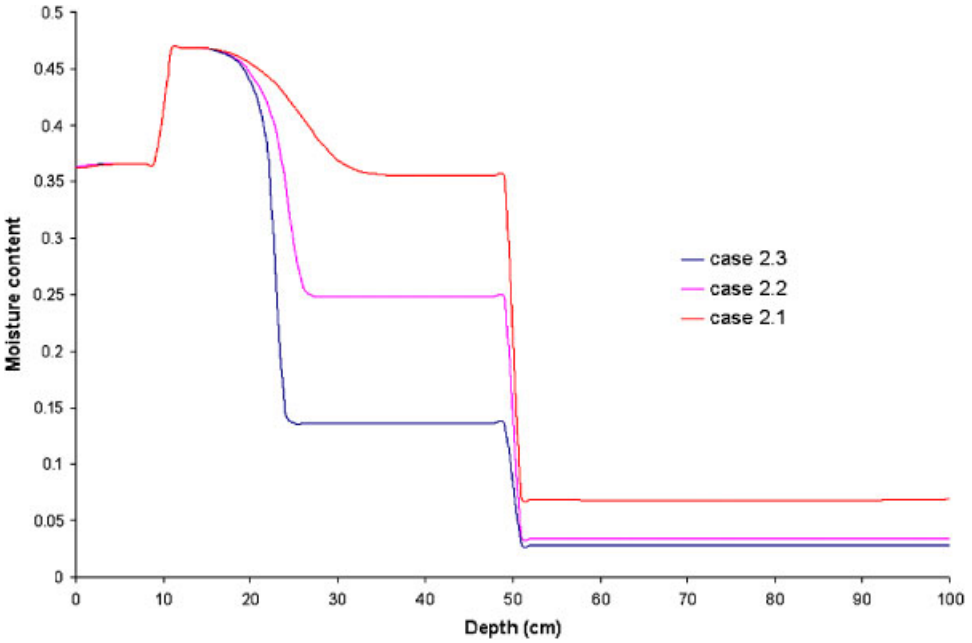

Figure 2. One-dimensional variably saturated flow (Case 5.1).

Table III. Number of time steps required with average time-step size in seconds given in brackets (Case 5.1).

Case	$\beta = 0.0$	$\beta = -0.02$	$\beta = -0.04$	$\beta = -0.06$
1.1	34 (423.5)	22 (654.5)	21 (685.7)	21 (685.7)
1.2	142 (202.8)	46 (626.1)	40 (720.0)	37 (778.4)
1.3	Not completed	83 (520.9)	74 (583.8)	72 (600.0)
2.1	61 (224.3)	33 (414.5)	27 (506.7)	25 (547.2)
2.2	212 (84.9)	58 (310.3)	44 (409.1)	37 (486.5)
2.3	Not completed	94 (229.8)	65 (332.3)	54 (400.0)

were run with and without applying the transformation. The sharp changes in the water pressure head resulted in the switching algorithm reverting to the mixed form in all the cases.

For the cases with very dry initial conditions, 1.3 and 2.3, the h-based method required an excessively small time-step size, of the order of 10^{-8}, to achieve convergence within 50 iterations. For all other cases the simulations run times were approximately 1 s for a mesh consisting of 100 elements on a PC with an AMD Athlon 1600 + 1.39 Ghz processor. Table III, gives the total number of time steps taken per simulation with the transformation parameter set to $\beta = 0.0$, $\beta = -0.02$, $\beta = -0.04$ and $\beta = -0.06$. The average time-step size in seconds is given in brackets. In all cases applying the transformation enabled convergent solution with much larger time steps. Setting $\beta = -0.04$ gave the fastest solutions as it required

the least number of iterations within a time step. Initially, small time steps were required as the solution penetrates the dry soil, after approximately 0.15 days the maximum time-step size of 900 s is reached and maintained until towards the end of the simulation when it reduces as the perched water table develops.

5.2. *Problem 2: one-dimension drainage*

This case involves vertical drainage through layered soil from initially saturated conditions. At time $t = 0$, the pressure head at the base of the column is reduced from 200 to 0 cm. During the subsequent drainage, a no-flow boundary condition is applied to the top of the column. Although a one-dimensional problem, it is a challenging test for a numerical method because of the sharp discontinuity in the moisture content that occurs at the interface between two material layers. During drain-down the middle coarse soil tends to restrict drainage from the upper fine soil and high saturation levels are maintained in the upper fine soil for a considerable period of time. Marinelli and Durnford [47] provide a semi-analytical solution to the problem. The hydraulic properties of the soils are given in Table IV. The Brooks–Corey model is used to prescribe the pressure–moisture relationship. The soil profile is soil 1 for $60\,\text{cm} > z > 0\,\text{cm}$ and $200\,\text{cm} > z > 120\,\text{cm}$, and soil 2 for $120\,\text{cm} > z > 60\,\text{cm}$, where z is the height of the column.

Simulations were performed on a fine mesh of 150 elements and a coarser mesh of 75 elements. The iterative procedure within a time step was considered converged when the difference in the water pressure head between two successive iterations fell below 10^{-4}. The switching algorithm reverted to the h-based form after the first couple of time steps. All transformed methods were in good agreement and the fine mesh solutions were in excellent agreement with the semi-analytical results of Marinelli and Durnford [47]. The simulation times ranged from 10 to 14 s, with the finer mesh simulation being slightly quicker as faster convergence was achieved within a time step. The simulations were also performed without the transformation, $\beta = 0$. The switching method, which reverted to the h-based form, required very small time steps to achieve convergence in the initial stages. The untransformed mixed method failed to achieve convergence with a minimum time-step size of 0.001 s. Figures 3 and 4 show the time-step size and number of iterations required to achieve convergence in a time step, for the transformed mixed, transformed switching algorithm and untransformed switching method. Figure 5 shows the saturation predictions along with the semi-analytical solutions at a time of 1 050 000 s (approximately 12 days).

Table IV. Soil hydraulic properties (Case 5.2).

	Soil 1 (fine soil)	Soil 2 (coarse soil)
θ_{sat}	0.35	0.35
θ_{res}	0.07	0.035
$\alpha\,\text{cm}^{-1}$	0.0286	0.0667
N	1.5	3.0
K_{sat} (cm/s)	9.81×10^{-5}	9.81×10^{-3}

Table V. Hydraulic properties of the soils (Case 5.3).

	Clay	Sand
θ_{sat}	0.4686	0.3658
θ_{res}	0.1060	0.0286
$\alpha\,\mathrm{m}^{-1}$	1.04	2.8
N	1.3954	2.239
K_{sat} (m/s)	1.516×10^{-6}	6.262×10^{-5}

Table VI. Simulation and CPU times for Case 5.3 (* initial results).

	$\beta = 0.0$	$\beta = -2.0$	$\beta = -4.0$	$\beta = -6.0$
Run time (s)	Not completed	111	91	199
No. of time steps	Not completed	1080	1080	1091
Average δt (s)	* Approx 10^{-6}	1000	1000	990

5.3. Problem 3: two-dimensional unsaturated flow into heterogeneous soil

The first two-dimensional problem is purely unsaturated flow into a region of clay and sand, Figure 6. The region is 5 m wide $\times$ 3 m deep divided into nine alternating blocks of clay and sand. A flux of water at 5 cm/day is applied across the middle of the top block of sand, 1 m wide. A zero-flux boundary condition is applied to all other boundary surfaces. The hydraulic properties of the soils are given in Table V. The van Genuchten model is used to prescribe the pressure–moisture relationship. The solution domain was meshed using a spatial step size of 5 and 2.5 cm giving a total of 12 000 and 24 000 elements and the simulation was run for 12.5 days. The moisture content and pressure head contours are shown in Figures 7 and 8, respectively, and compare well to those published in References [15, 29]. To compare the accuracy with respect to flux, the vertical flux at, $x = 2.55$ m, and horizontal flux at, $y = 0.95$ m, are plotted along side the very dense grid solutions (using spatial step size of 1 cm) of Pan and Wierenga in Figures 9 and 10, respectively. The solutions obtained using a coarse grid is in excellent agreement with the very dense grid.

The coarse grid simulation was run using a transform parameter of $\beta = 0.0$, $\beta = -2.0$, $\beta = -4.0$ and $\beta = -6.0$. Applying no transformation required a very small time step, in the order of 10^{-6}, to achieve convergence within a maximum of 30 iterations. When a transformation was employed all simulations converged well and the moisture content and pressure head results were all in agreement. The simulation run times on a PC with and with AMD Athlon 1600 + 1.39 Ghz processor are given in Table VI along with number of time steps and average time-step size, δt. Using a transformation dramatically improved convergence and enabled much larger time-step sizes to be employed, a maximum time-step size of 1000 s was specified. The maximum time-step size was employed for transformation parameters of $\beta = -2.0$ and $\beta = -4.0$. For $\beta = -6.0$ the simulation initially required a smaller time-step size of 110 s which increased to 1000 s over the first three simulated hours. The transformation parameter of $\beta = -4.0\,\mathrm{m}^{-1}$ required the least number of iterations to achieve convergence and had the fastest simulation time.

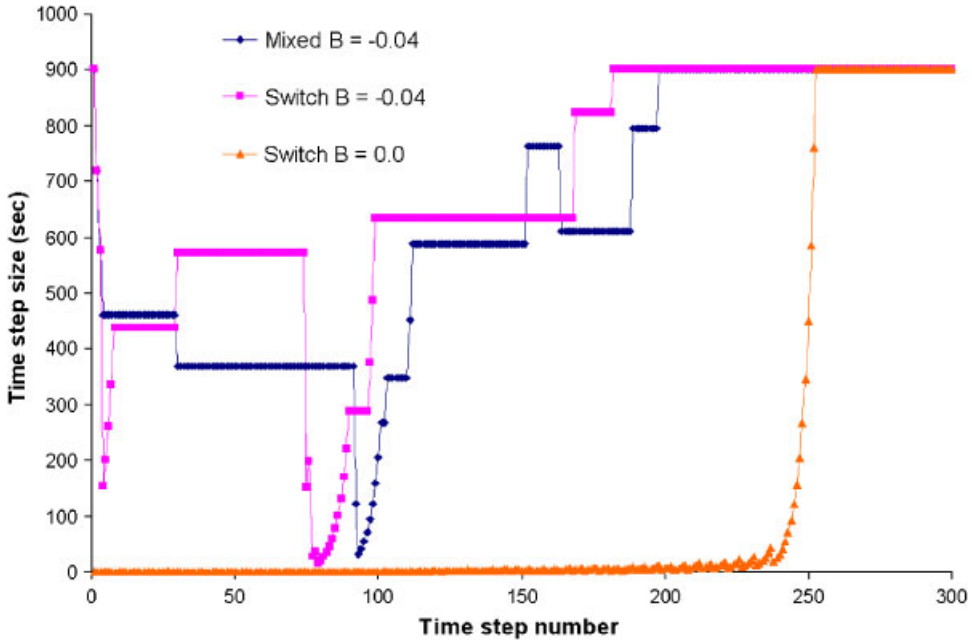

Figure 3. Time-step size employed in mixed, transformed and untransformed switching algorithm.

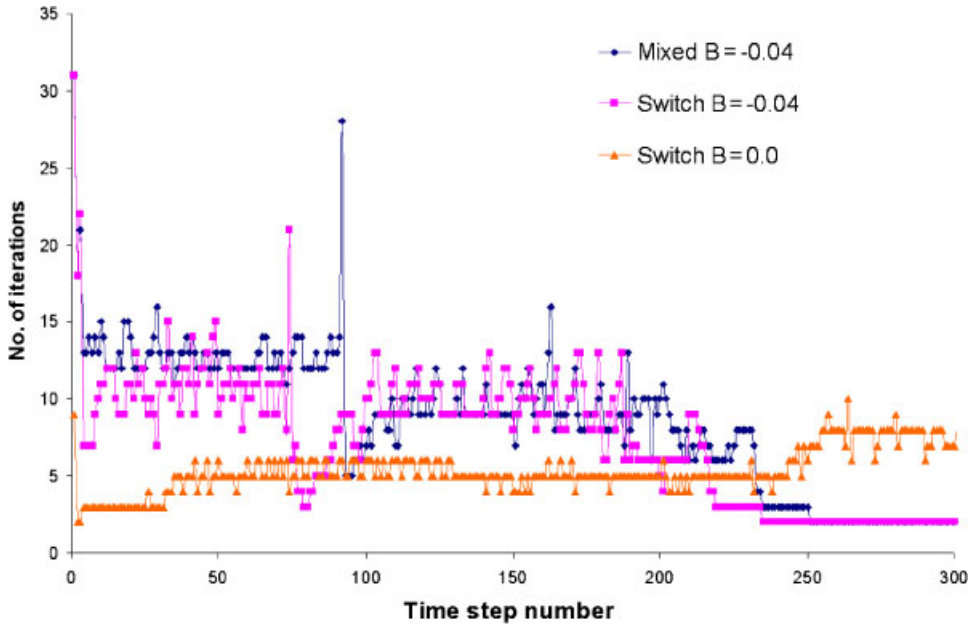

Figure 4. Number of iterations required within a time step for converging solutions for mixed and switching algorithm.

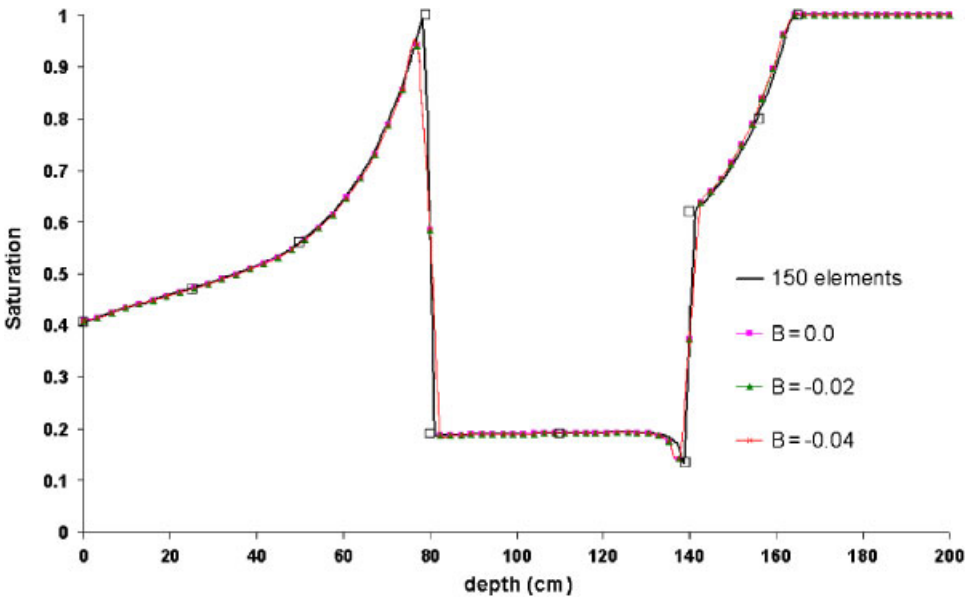

Figure 5. Saturation predictions after approximately 12 days for Case 5.2.

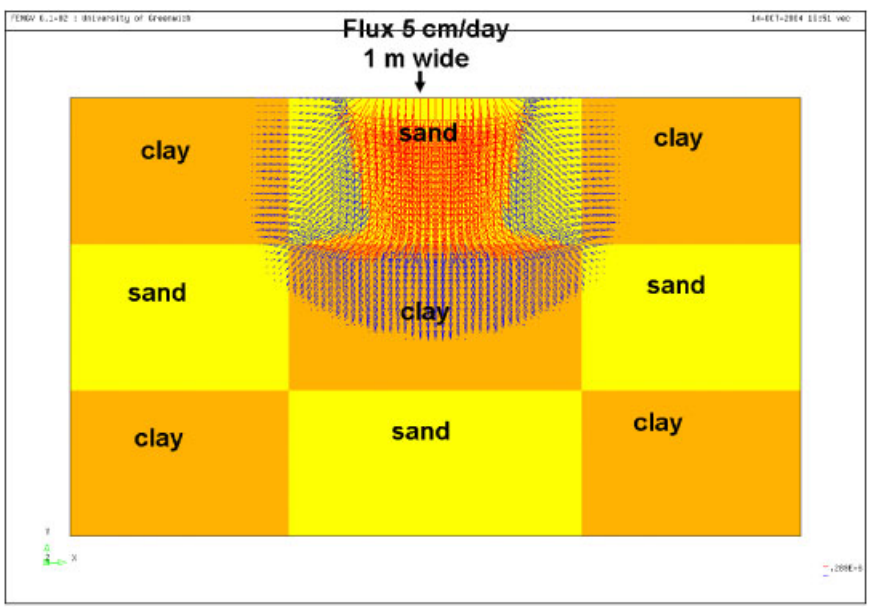

Figure 6. Unsaturated flow into heterogeneous soil, showing resultant flux vectors after 12.5 days.

Figure 7. Saturated contour plot after 12.5 days.

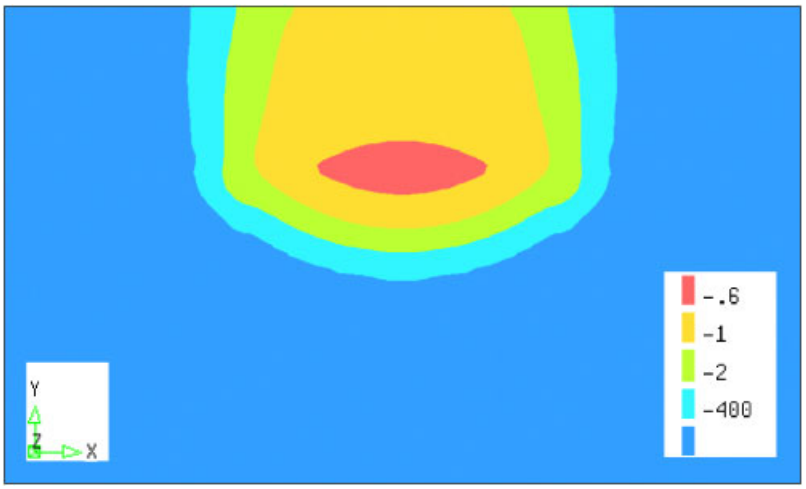

Figure 8. Contour pressure head (in m) after 12.5 days.

5.4. *Problem 4: two-dimensional variably saturated flow*

The second two-dimensional test problem involves flow into initially very dry layered soil of sand and clay with a developing water table. The hydraulic properties of the sand and clay are taken as Case 1, given in Table I. To achieve a perched water table, a 3 m × 1 m region of sand was bounded by clay, as shown in Figure 11. A water flux rate of 50 cm per day

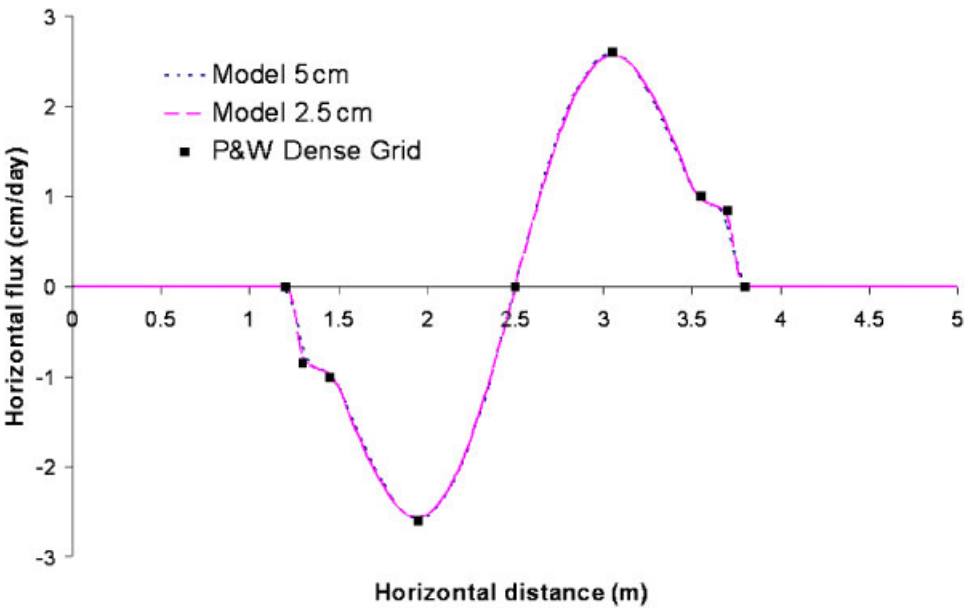

Figure 9. Horizontal flux at depth 0.95 m for unsaturated case after 12.5 days.

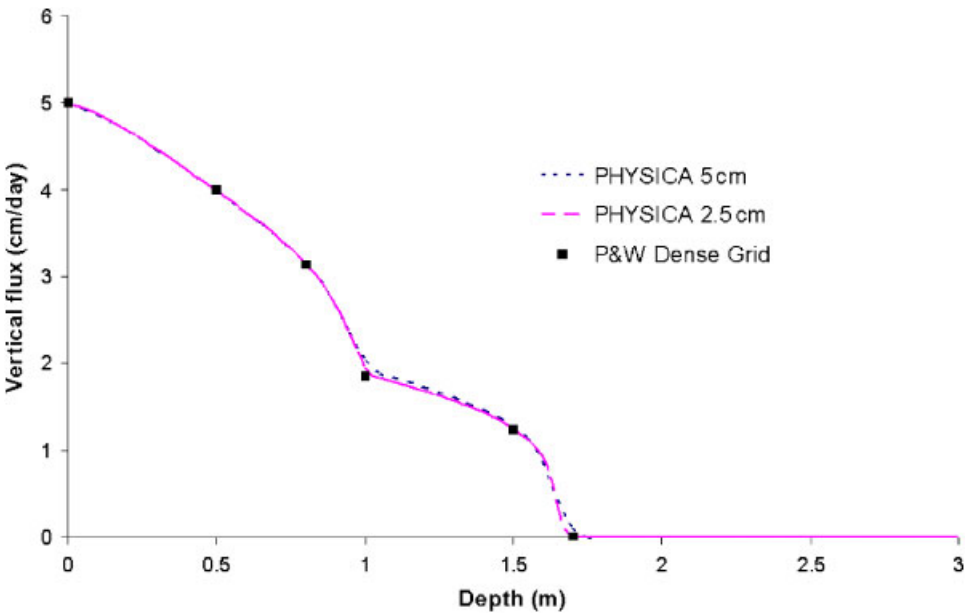

Figure 10. Vertical flux at $x = 2.55$ m for unsaturated case after 12.5 days.

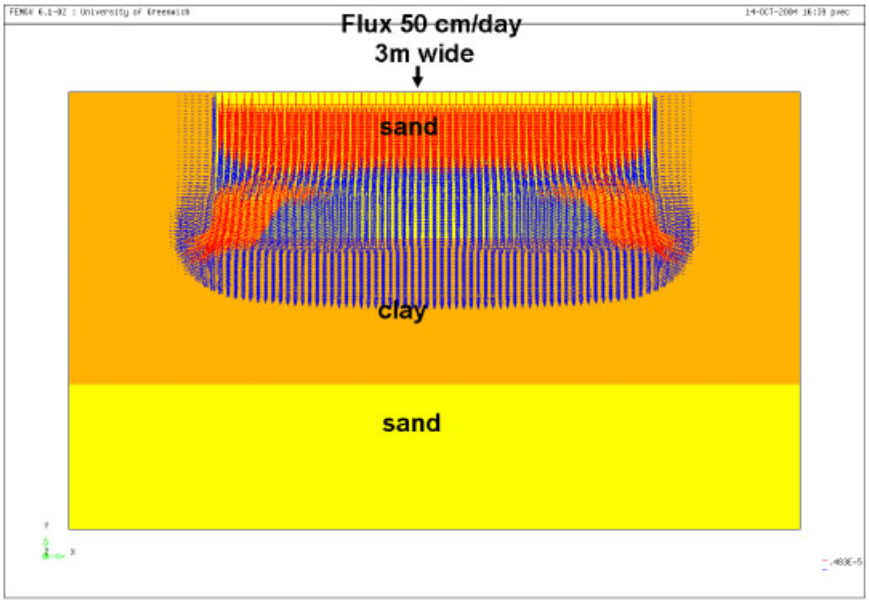

Figure 11. Geometry of perched water table problem showing resultant flux vectors after 1 day.

Table VII. Simulation and CPU times for Case 5.4 (* initial results).

	$\beta = 0.0$	$\beta = -2.0$	$\beta = -4.0$	$\beta = -6.0$
Run time (s)	Not completed	1036	15	16
No. of time steps	Not completed	2780	98	98
Average δt (s)	* Approx 10^{-6}	31	882	882

was applied to the top sand surface and the simulation period was one day. A uniform mesh consisting of 6000 and 12 000 elements with a spatial step size of 5 and 10 cm, respectively, was used in the simulation. This perched water table problem is a difficult case to simulate. The case was simulated using a transformation parameter β of 0, -2 and $-4\,\mathrm{m}^{-1}$. Convergence problems were encountered with zero transformation and very small time steps were required, in the order of 10^{-6} s. A transformation parameter of $\beta = -2\,\mathrm{m}^{-1}$ improved convergence, but increasing the value of β to -4 and $-6\,\mathrm{m}^{-1}$ gave fast converging solutions with much larger time-step sizes. Table VII gives the simulation run times, number of time steps and average time-step size, δt. The highly non-linear nature of the problem meant that more iterations were required per time step to achieve convergence than for the purely unsaturated flow problem.

The contour plots of saturation and pressure head are shown in Figures 12 and 13, respectively. All completed simulations gave comparable predictions that agree well with published results [15, 17, 29]. After approximately half a day, a water table begins to develop

Figure 12. Saturation levels after one day.

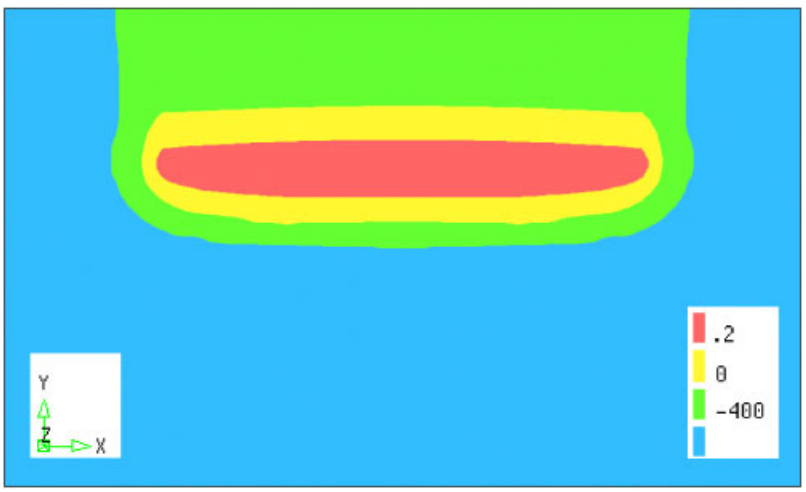

Figure 13. Pressure head contour after one day.

at the interface of the sand and clay layers, at a depth of approximately 1 m. Figures 14 and 15 show the fluxes, the vertical flux at, $x = 2.55$ m, and horizontal flux at, $y = 0.95$ m, plotted along side the very dense grid solutions of Pan and Wierenga. All solutions obtained are in good agreement with the dense grid solutions.

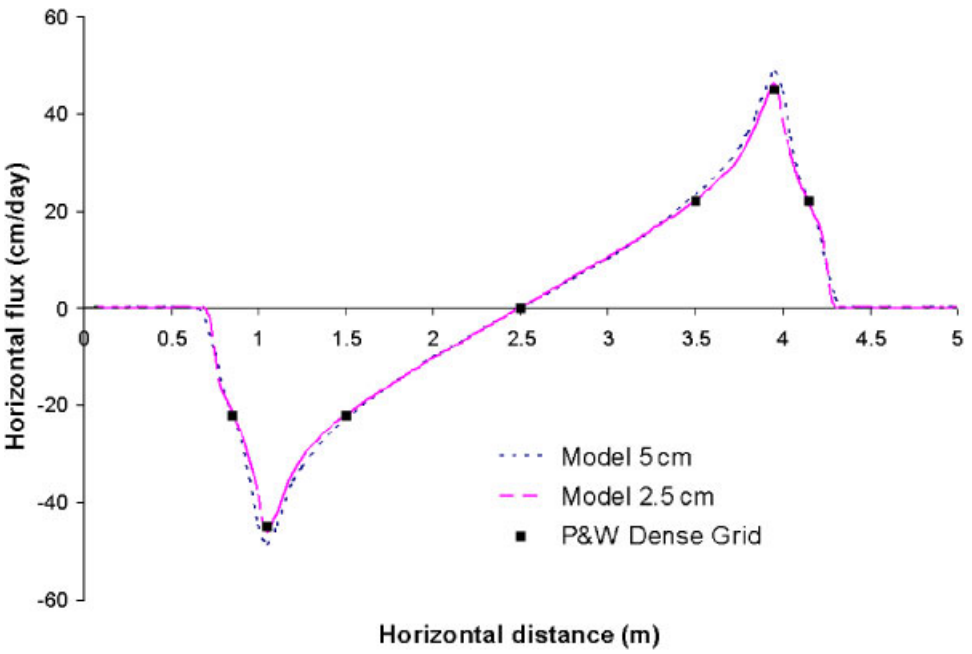

Figure 14. Horizontal flux at depth 0.95 m for variably saturated case after one day.

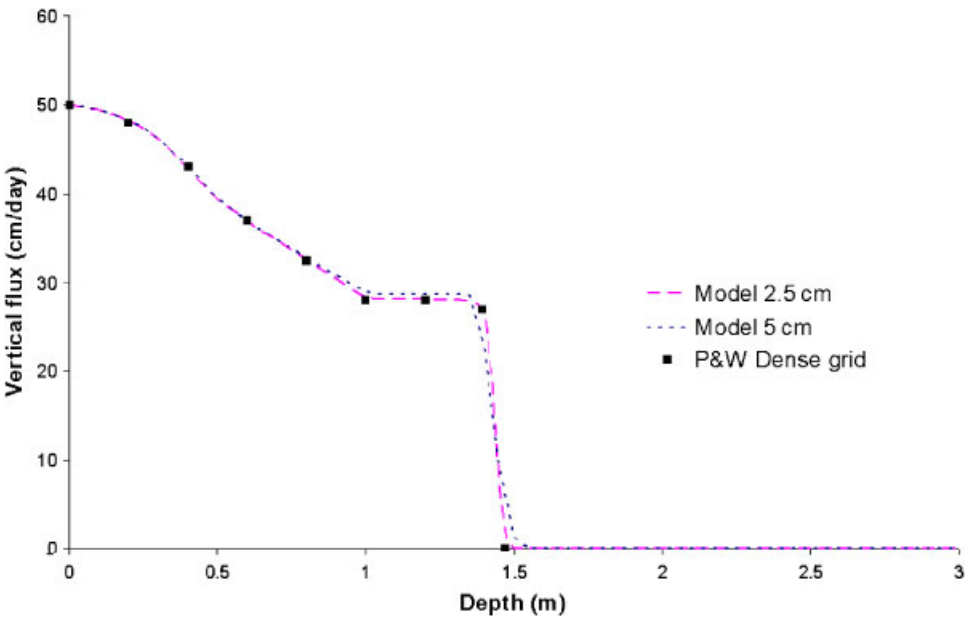

Figure 15. Vertical flux at $x = 2.55$ m for variably saturated case after one day.

6. THREE-DIMENSIONAL FLOW CASE

Finally, the flow algorithm is illustrated on a three-dimensional mesh drawn from an ore heap-leaching problem. The mesh, geometry and dimensions of the domain are shown in Figure 16. The mesh consists of 24 000 hexahedral elements. There is an inlet positioned at the centre front of the top surface and two outlets positioned at the back of the bottom surface. The inlet surface area is $1\,\mathrm{m} \times 1\,\mathrm{m}$; the outlet surface areas are both $0.5\,\mathrm{m} \times 1\,\mathrm{m}$. All other surfaces assume a no-flux boundary condition. The van Genuchten parameters for the ore are, $\alpha = 4\,\mathrm{m}^{-1}$ and $N = 3$. The simulation is run for 21 days. Three cases were considered, the first two cases assume homogeneous ore with an effective permeability of $2.5 \times 10^{-7}\,\mathrm{m/s}$ at an ore moisture content of 12%. In the first case a constant flux of $1.7 \times 10^{-6}\,\mathrm{m/s}$ of water is applied to the inlet surface for a 7-day period. In the second case a constant flux of $2.7 \times 10^{-6}\,\mathrm{m/s}$ is applied to the inlet surface for the full 21-day period to achieve saturated conditions at the base of the heap. In the final case a block, dimensions $2\,\mathrm{m} \times 1\,\mathrm{m} \times 1\,\mathrm{m}$, of low-permeability ore, with effective permeability of $2.5 \times 10^{-10}\,\mathrm{m/s}$ at an ore moisture content of 12%, was inserted into the central front area of the domain. A constant flux of $2.7 \times 10^{-6}\,\mathrm{m/s}$ is applied for the full 21-day period. For all simulations, very dry initial conditions were assumed, with a 6% initial moisture level.

6.1. *Homogeneous case-unsaturated*

Saturation contour plots for the first homogeneous case are shown in Figure 17, at 1, 7, 14 and 21 days. A flux is applied to the inlet surface for 7 days; the moisture content builds up in the area below the inlet reaching a maximum saturation level of 0.95 on day 10. After the flux is turned off on day 7, the saturation levels continue to increase slightly at the base over the next 3 days and then gradually reduce as the solution drains through the outlets. After 21 days the area directly under the inlet at the base of the geometry has a maximum saturation level of 70%. The resultant flux vectors on day 2, 4, 6 and 8 are shown in Figure 18.

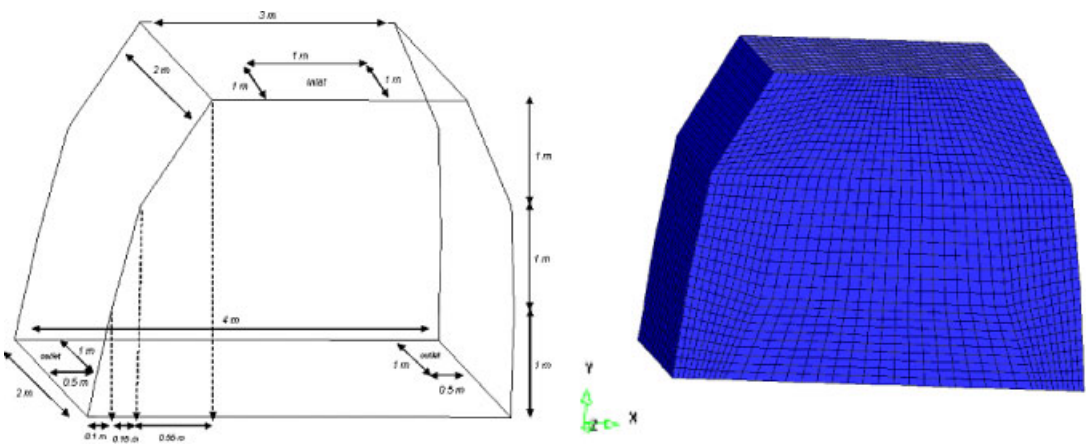

Figure 16. Geometry of heap and three-dimensional mesh.

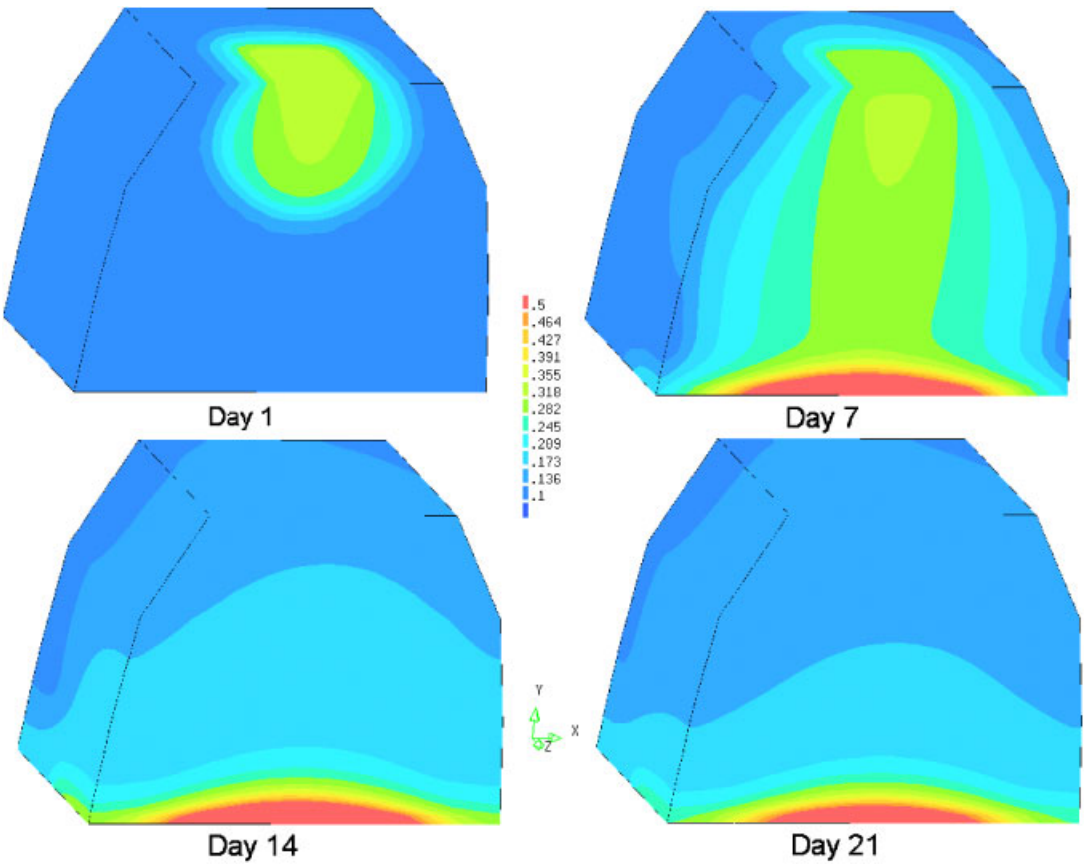

Figure 17. Saturation contour plots for homogeneous unsaturated flow.

6.2. *Homogeneous case—variably saturated flow*

In the second case the solution is applied to the homogeneous material for the full 21-day simulation period, giving regions with fully saturated conditions, as illustrated in Figure 19. The solution travels freely down to the base of the domain, where saturation levels build in the area under the inlet surface. Fully saturated conditions are encountered in the base area after approximately 7 days, see Figure 20.

6.3. *Heterogeneous case—variably saturated flow*

Finally, the solution is applied for heterogeneous material with a low-permeability region, in the centre front of the geometry, at a distance of 1 m under the inlet surface. Figure 21 shows the saturation levels in the domain at day 1, 7, 14 and 21. The low-permeability region prevents the solution from travelling straight through the domain and an area under the block of low-permeability material remains solution free for a long period of time. After

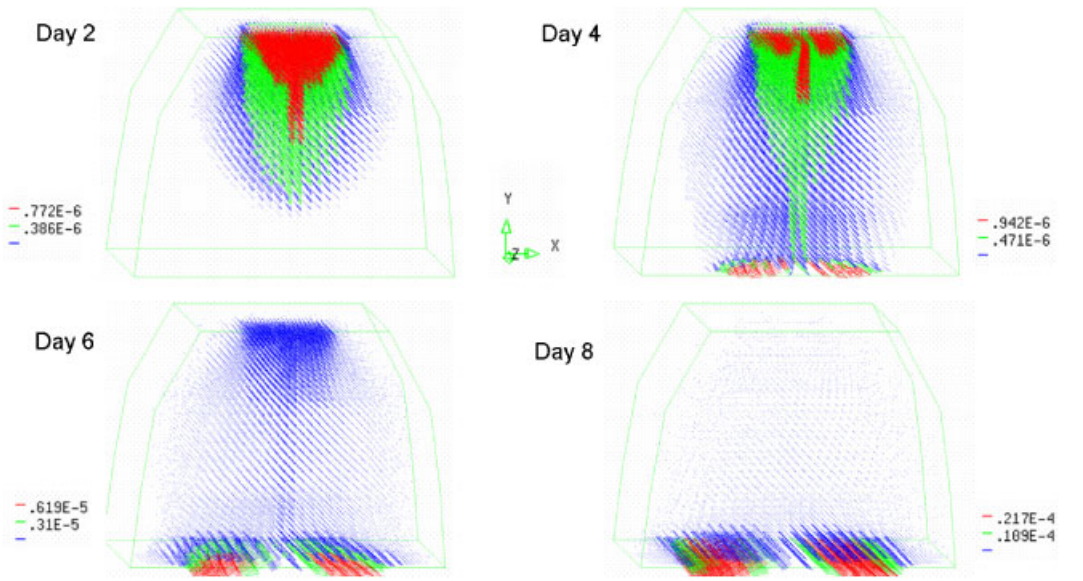

Figure 18. Flux vector plots for homogeneous unsaturated flow.

5-days application of the area at the top of the low-permeability region has neared saturation. Saturation at the base of the heap occurs on day 9. The maximum saturation level in the low-permeability material is 0.95 at the top region and over next two-week period the moisture gradually spreads through the region of low permeability to a maximum of 0.5 in the lower region. Figures 22 and 23 show the resultant flux as it encounters the region of low permeability and the solution chooses the route of highest permeability.

The solution recovered though the outlets are shown in Figure 24 for constant flux homogeneous and heterogeneous cases. Solution is initially recovered on day 4 for the homogeneous material and day 5 for the heterogeneous case.

6.4. Computational performance

The CPU times for the solution of flow can be approximated from the three-dimensional test cases. All simulations were performed on a Pentium 4, 2.50 GHz-M processor. The mesh used in the three-dimensional simulations comprised of 24 000 hexahedral elements. The memory requirements were 5.24 megabytes, giving an approximate memory demand per mesh element of 229 bytes. The simulation time for both the homogeneous unsaturated flow cases was approximately 16 min. The simulations, involving variably saturated flow, required 8 and 14 min for the homogeneous and heterogeneous cases, respectively. CPU time will vary to some extent depending upon the complexity of the problem, e.g. whether layered material or perched water tables are involved.

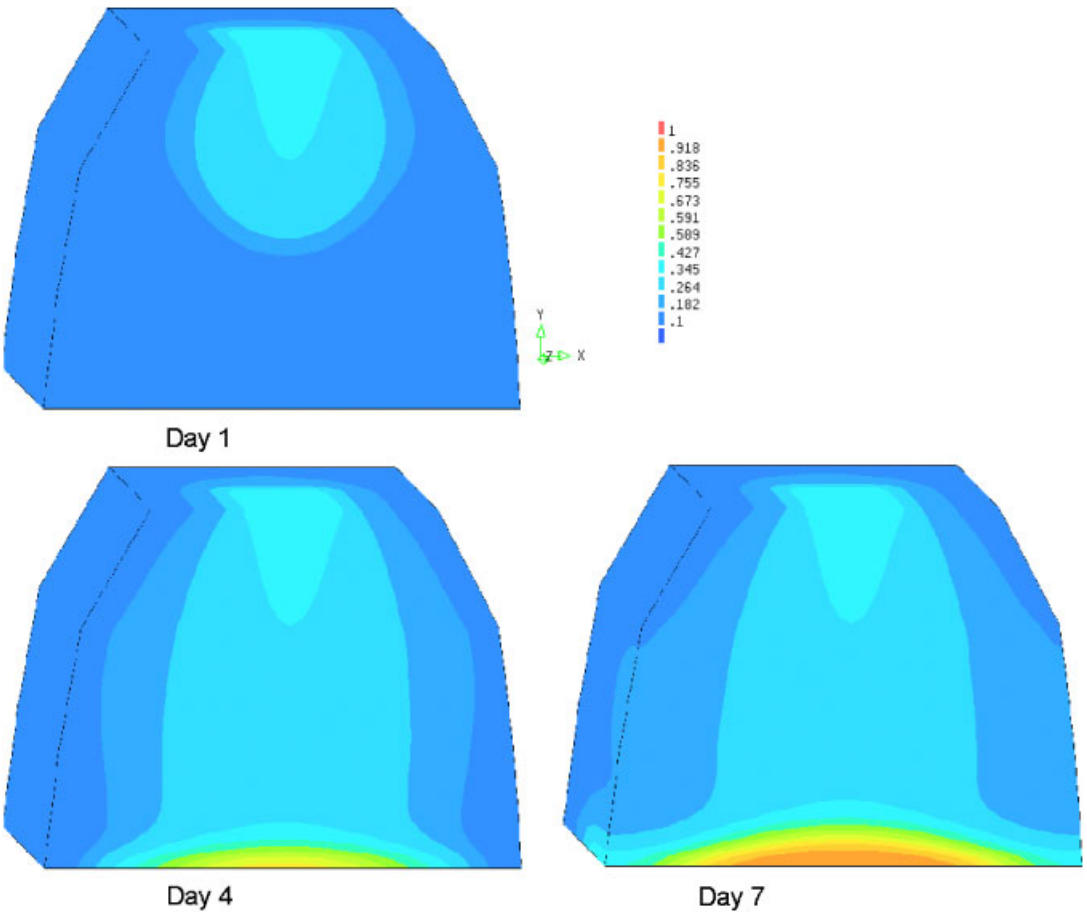

Figure 19. Saturation levels, homogeneous—variably saturated flow.

7. CONCLUSION

The objectives of the first phase of our heap-leaching modelling research programme included the development and implementation of a numerical procedure for the effective simulation of liquid flow through porous media under variably saturated conditions within complex three-dimensional geometries, in the context of conventional commercially supported general-purpose finite-volume-based CFD codes using cell-centred discretization techniques on three-dimensional unstructured meshes. This contribution describes the design, implementation, testing and evaluation of an effective procedure for the simulation of variably saturated flow in porous media with spatially varying properties. The procedure involves:

- The transformation variable first defined by Pan and Wierenga that eliminates the sharp discontinuity at the moisture interface.

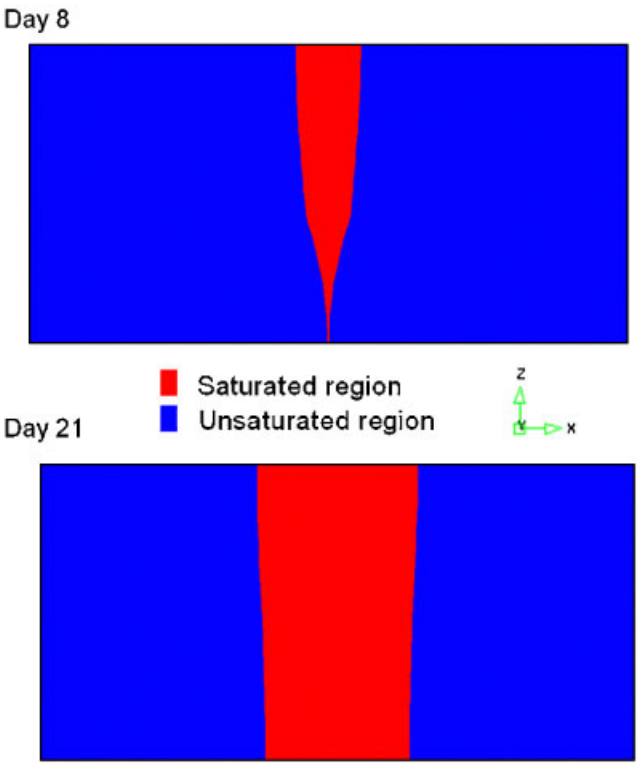

Figure 20. Saturation at base, homogeneous—variably saturated flow.

- A simple switching method between the mixed Picard iteration scheme and the standard *h*-based Picard iteration proposed by Hao *et al.* for efficient long time simulations of water flow in soils with frequent infiltration and deep drainage processes.
- A fully implicit finite volume discretization on a fixed unstructured mesh using tetrahedral up to hexahedral elements where approximations are cell centred (i.e. the control volume equals the element volume) with a diagonally pre-conditioned conjugate-gradient solver for the transformed pressure head.
- Adaptive time stepping to ensure convergence and CPU efficiency.
- The structuring of the procedure to enable the inclusion of any pressure head–moisture saturation level relationship–van Genuchten and Brooks–Corey are included as standard.
- The implementation of the algorithm within the PHYSICA computational modelling software framework for multi-physics simulation.
- An evaluation of the procedure on a range of test problems that provide challenges at the physical extremes of variably saturated flow characteristics.
- A demonstration of the model in analysing a three-dimensional geometry and flow conditions similar to those of flow through leached heaps.

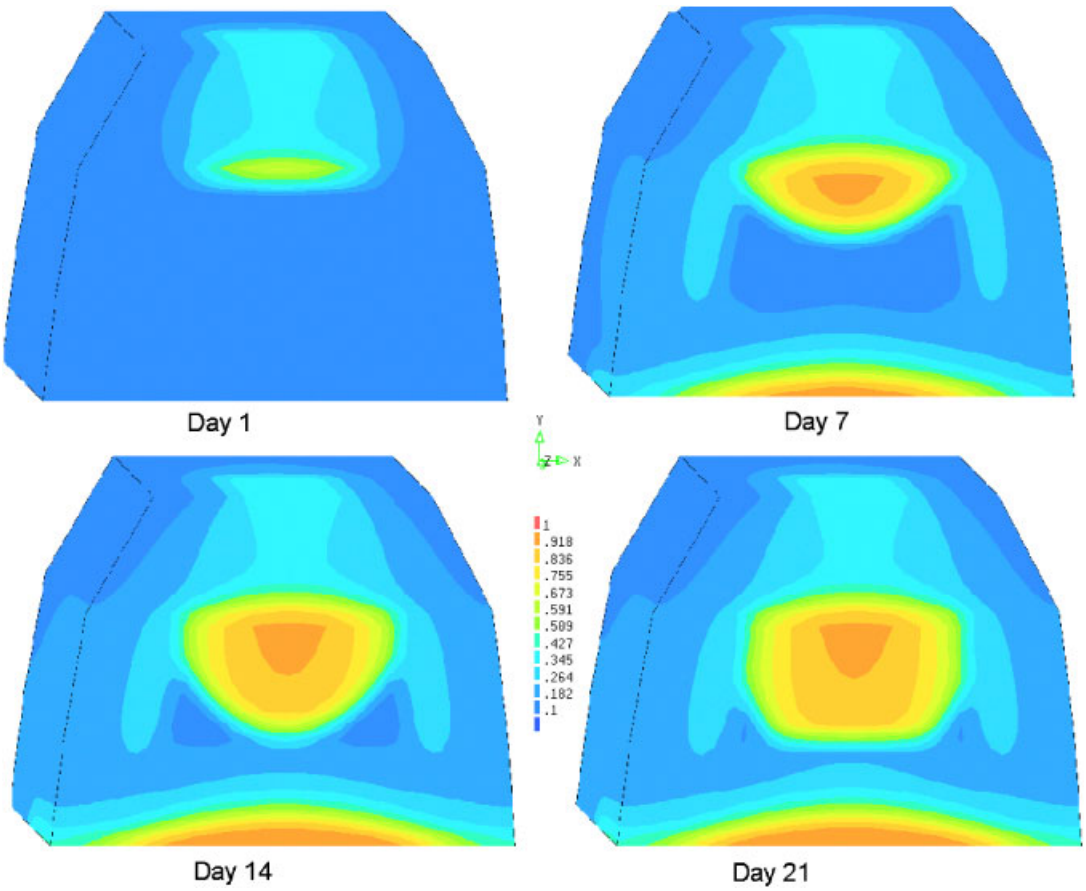

Figure 21. Saturation levels, heterogeneous material.

In summary, the model flow algorithm:

- Solved *accurately and with computational efficiency*, some discriminating tests cases involving relatively extreme conditions with regard to (a) initial dry conditions, (b) sharp boundaries between the unsaturated and saturated conditions, and to drainage scenarios.
- Shows the *enhanced convergence* behaviour of the transformed equations, enabling solutions on a much coarser mesh and employing larger time steps.
- Is *comprehensive* (in that it is structured to represent any kind of porous flow model; Brooks–Corey and van Genuchten are implemented as standard options).
- Has been *demonstrated* on a basic three-dimensional geometry to indicate its potential as the basis for heap-leach modelling. Not only did the model solve the problems in a robust fashion, but the procedure was also computationally efficient, in simulating 30 days behaviour in less than 20 min on a conventional PC processor.

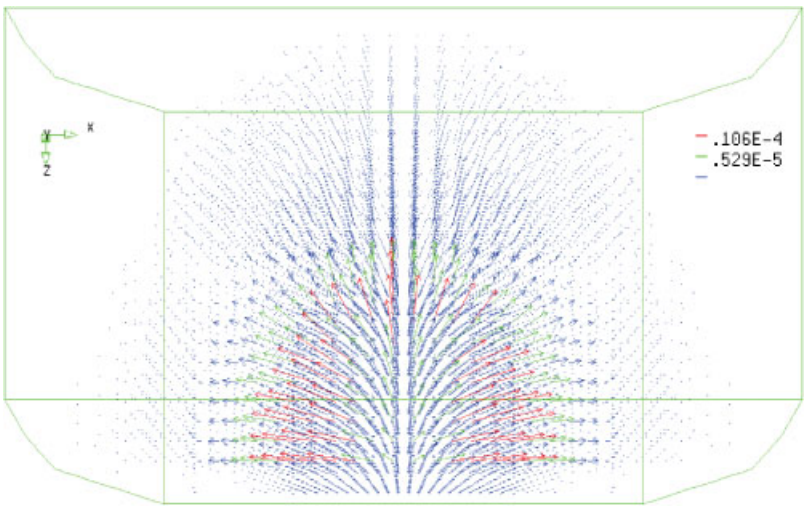

Figure 22. Flux vectors on day 3, heterogeneous material.

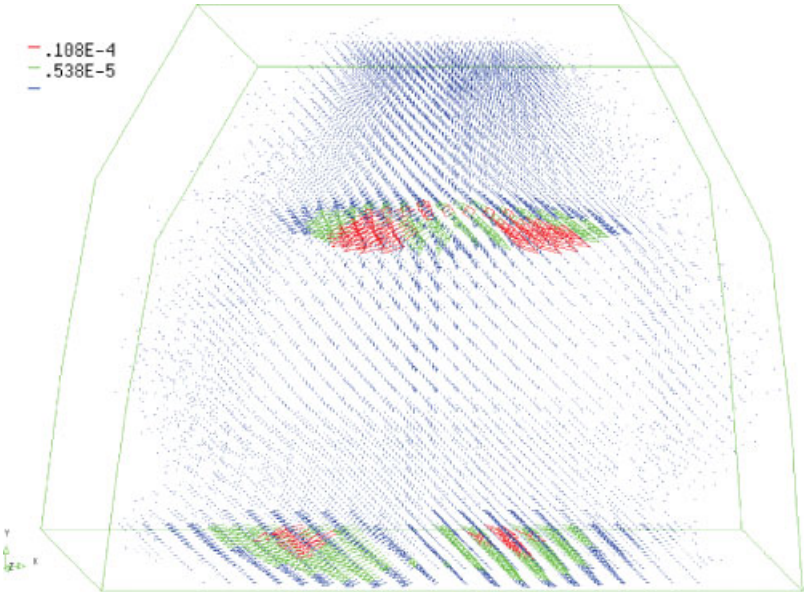

Figure 23. Flux vectors on day 5, heterogeneous material.

Other aspects of the heap-leach modelling programme have involved the design and implementation of the reaction models to characterize the extraction rates as a function of local conditions and predict the behaviour of the pregnant solution as it exits the heap, see, for example, References [48, 49]. A further stage will involve incorporating the variably saturated

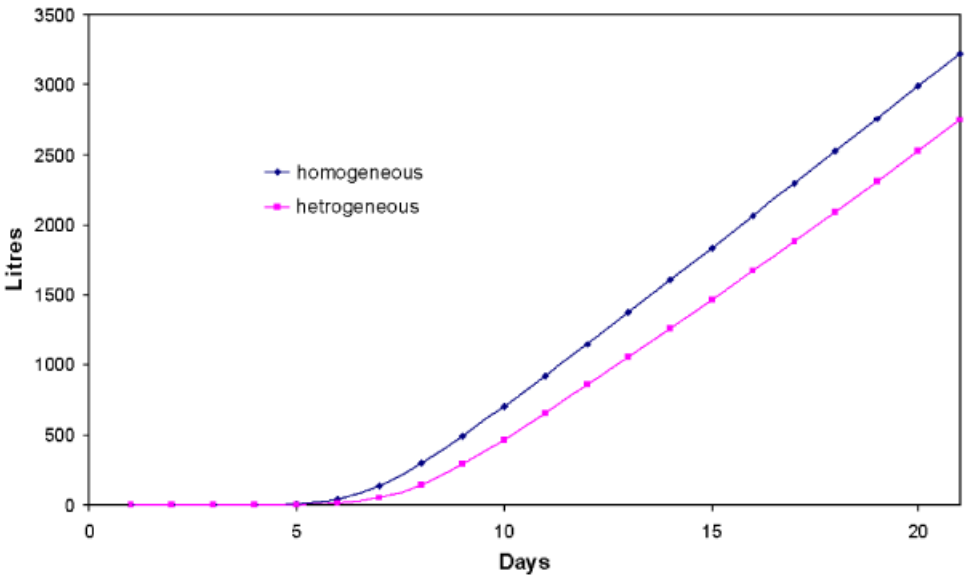

Figure 24. Recovered solution.

flow algorithm described above within the heap-leaching models currently under development and their evaluation on high-performance parallel clusters.

REFERENCES

1. Simunek J, Huang K, van Genuchten MT. The SWMS-3D code for simulating water flow and solute transport in three-dimensional variably saturated media. *Research Report No. 139*, US Salinity Lab., Riverside, CA, 1995.
2. 3D FEMFAT. See www.scisoftware.com
3. SVFLUX. See www.svflux.com
4. Yeh GT. *FEMWATER*: *A Finite Element Model of Water Flow through Saturated-Unsaturated Porous Media* (ORNL-5567/RI edn). Oak Ridge National Laboratory: Oak Ridge, TN.
5. FLUENT. http://www.fluent.com
6. CFX. http://www.ansys.com/cfx
7. STAR-CD. http://www.cd-adapco.com
8. Bartlett RW. *Solution Mining* (2nd edn). Gordon & Breach, Science Published: Amsterdam, The Netherlands, 1998.
9. PHYSICA+. See http://www.physica.co.uk
10. Celia MA, Bouloutas ET, Zarba RL. A general mass-conserved numerical solution for the unsaturated flow equation. *Water Resources Research* 1990; **26**:1483–1496.
11. Milly PCD. A mass-conservative procedure for time-stepping in models of unsaturated flow. *Advances in Water Resources* 1985; **8**:26–32.
12. Pan L, Warrick AW, Wierenga PJ. Finite element methods for modelling water flow in variably saturated porous media: numerical oscillation and mass-distributed schemes. *Water Resources Research* 1996; **32**:1883–1889.
13. Tocci MD, Kelley CT, Miller CT. Accurate and economical solutions of the pressure-head form of Richards equation by the method of lines. *Advances in Water Resources* 1997; **20**:1–14.
14. Hills RG, Porro I, Hudson DB, Wierenga PJ. Modeling one-dimensional infiltration into very dry soils, model development and evaluation. *Water Resources Research* 1989; **25**(6):1259–1269.
15. Kirkland MR, Hills RG, Wierenga PJ. Algorithms for solving Richards equation for variably saturated soils. *Water Resources Research* 1992; **28**:2049–2058.
16. Forsyth PA, Wu YS, Pruess K. Robust numerical methods for saturated-unsaturated flow with dry initial conditions in heterogeneous media. *Advances in Water Resources* 1995; **18**:25–38.

17. Diersch HJG, Perrochet P. On the primary variable switching technique for simulating unsaturated-saturated flows. *Advances in Water Resources* 1999; **23**:271–301.
18. Celia MA, Bining P. A mass-conservative numerical solution for two-phase flow in porous media with application to unsaturated flow. *Water Resources Research* 1992; **28**:2819–2828.
19. Huang K, Mohanty BP, van Genuchten MTh. A new convergence criterion for the modified iteration method for solving the variably saturated flow equation. *Journal of Hydrology* 1996; **178**:69–91.
20. Gui S, Zhang R, Turner JP, Xue X. Probabilistic slope stability analysis with stochastic soil hydraulic conductivity. *Journal of Geotechnical Engineering* (ASCE) 2000; **126**:1–8.
21. Hao X, Zhang R, Kravchenko A. A mass-conservative switching method for simulating saturated-unsaturated flow. *Journal of Hydrology* 2005; **xx**:1–12.
22. Kavetski D, Binning P, Sloan SW. Adaptive time stepping and error control in a mass conservative numerical solution of the mixed form of Richards equation. *Advances in Water Resources* 2001; **24**:595–605.
23. Abriola LM, Lang JR. Self-adaptive finite element solution of the one-dimensional unsaturated flow equation. *International Journal for Numerical Methods in Fluids* 1990; **10**:227–246.
24. Forsythe PA. A control volume finite element method for local mesh refinement. *10th Society of Petroleum Engineers Symposium on Reservoir Simulation*, *Paper 18415*, Society of Petroleum Engineering, Richardson, TX, 1989.
25. Hornung RD, Trangenstein JA. Adaptive grid refinement and multilevel iteration for flow in porous media. *Journal of Computational Physics* 1997; **136**:522–545.
26. Mansell RS, Ahuja LR, Bloom SA. Adaptive grid refinement in numerical models for water flow and chemical transport in soil: a review. *Vadose Zone Journal* 2002; **1**:222–238.
27. Haverkamp R, Vauclin M, Touma J, Wierenga PJ, Vachaud G. Comparison of numerical simulation models for one-dimensional infiltration. *Soil Science Society of America Journal* 1977; **41**:285–295.
28. Ross PJ. Cubic approximation of hydraulic properties for simulations of unsaturated flow. *Water Resources Research* 1992; **28**:2617–2620.
29. Pan L, Wierenga PJ. A transformed pressure head-based approach to solve Richards equation for variably saturated soils. *Water Resources Research* 1995; **31**:925–931.
30. Williams GA, Miller CT, Kelley CT. Transformation approaches for simulating flow in variably saturated porous media. *Water Resources Research* 2000; **36**:923–934.
31. Pan L, Wierenga PJ. Improving numerical modelling of two-dimensional water flow in variably saturated, Heterogeneous porous media. *Soil Science Society of America Journal* 1997; **61**:335–346.
32. Williams GA, Miller CT. An evaluation of temporally adaptive transformation approaches for solving Richards equation. *Advances in Water Resources* 1999; **22**(8):831–840.
33. Simunek J, Vogel T, van Genuchten MT. The SWMS-2D code for simulating water flow and solute transport in two-dimensional variably saturated media. *Research Report No. 126*, US Salinity Laboratory, Riverside, CA, 1992.
34. Yeh GT. *FEMWATER*: *A Finite Element Model of Water Flow through Saturated-Unsaturated Porous Media* (ORNL-5567/RI edn). Oak Ridge National Laboratory: Oak Ridge, TN.
35. Simunek J, Huang K, Segna M, van Genuchten MTh. *The HYDRUS-1D Software Package for Simulating the One-dimensional Movement of Water Heat and Multiple Solutes Variably Saturated Media*, *Version 1.0*. US Salinity Laboratory, USDA/ARS: Riverside, CA, 1997.
36. Swaminathan CR, Voller VR. Towards a general numerical method for analysis of solidification systems. *International Journal of Heat and Mass Transfer* 1997; **40**:2859–2868.
37. Voller VR. An overview of numerical methods for phase change problems. *Advances in Numerical Heat Transfer* 1996; **1**:341–375.
38. Huang W, Zhan X, Zheng L. Adaptive moving mesh methods for simulating one-dimensional groundwater problems with sharp moving fronts. *International Journal for Numerical Methods in Engineering* 2002; **54**:1579–1603.
39. Manzini G, Ferraris S. Mass-conservative finite volume methods on 2-D unstructured grids for the Richards equation. *Advances in Water Resources* 2004; **27**:1199–1215.
40. Voller VR. A control volume finite element solution of the unsaturated flow equations in layered soils. *Computer Methods in Water Resources* 2002.
41. Rees I, Masters I, Malan AG, Lewis RW. An edge-based finite volume scheme for saturated-unsaturated groundwater flow. *Computer Methods in Applied Engineering* 2004; **193**:4741–4759.
42. Brooks RH, Corey AT. Hydraulic properties of porous media. *Hydrology Paper No. 3*, Civil Engineering, Colorado State University, 1964.
43. van Genuchten MT. A closed form equation for predicting the hydraulic conductivity of unsaturated soils. *Soil Science Society of America Journal* 1980; **44**:892–898.
44. Croft N, Pericleous KA, Cross M. PHYSICA: a multi-physics environment for complex flow processes. In *Numerical Methods in Laminar and Turbulent Flow '95*, Taylor C, Durbetaki P (eds), vol. 2, 1995; 1269–1280.

45. Patankar SV. *Numerical Heat Transfer and Fluid Flow*. McGraw-Hill: New York.
46. Rhie CM, Chow WL. Numerical study of the turbulent flow past an aerofoil with trailing edge separation. *AIAA Journal* 1983; **21**(11):1525–1532.
47. Marinelli F, Durnford DS. Semi analytical solution to Richards equation for layered porous media. *Journal of Irrigation and Drainage Engineering* 1998; **124**:290–299.
48. Bennett CR, Cross M, Croft TN, Uhrie JL, Green CR, Gebhardt J. A comprehensive copper stockpile leach model: background and model formulation. *CD-Proceedings of 2003 TMS/CIM Symposium on Hydrometallurgy*, Vancouver, August 2003.
49. Bennett CR, Cross M, Croft TN, Uhrie JL, Green CR, Gebhardt J. A comprehensive copper stockpile leach model: background and model sensitivity. *CD-Proceedings of Copper 2003—Cobre 2003 TMS Symposium*, Santiago, Chile, November 2003.

